LA-13830-MS

Backward Integration of a VISAR Record: Free-Surface to the Spall Plane

Los Alamos
NATIONAL LABORATORY

Los Alamos National Laboratory is operated by the University of California for the United States Department of Energy under contract W-7405-ENG-36.

LA-13830-MS

Issued: May 2001

Backward Integration of a VISAR Record: Free-Surface to the Spall Plane

Dennis Hayes
John Vorthman
Joe Fritz

Los Alamos
NATIONAL LABORATORY
Los Alamos, New Mexico 87545

Backward Integration of a VISAR Record: Free Surface to the Spall Plane

by

Dennis Hayes, John Vorthman, and Joe Fritz

Abstract

Plane shock and release waves are routinely used to produce spall fracture. Interpretation of measurements of the free-surface motion that contain detailed information on the spall process has been inhibited by the requirement that a spall model be assumed before experiment and theory can be compared. Using a modification of a technique initially developed at Sandia National Laboratories, we solve the equations of motion by using the free-surface motion as an "initial condition" and integrate back in space to the interior of the sample. In one experiment on aluminum, the interior location at which the late-time stress oscillations are minimized agrees well with the spall location estimated by other means. These late-time oscillations can almost be eliminated by treating the aluminum as a quasielastic material. The dislocation parameters that minimize the late-time root-mean-square stress are in substantial agreement with those determined by Johnson *et al.* for this material. Instabilities that occur in this latter set of parabolic equations are managed using numerical smoothing. Accuracy of the backward integration is checked by doing a forward integration using traditional techniques (those that do not depend on a potentially unstable equation set) to see if the original free-surface motion is recovered.

I. INTRODUCTION

The backward method of integrating the equations of motion (Backward) was developed at Sandia National Laboratories as an aid in interpreting VISAR[1] measurements made on the Z-Accelerator[2]. A typical Sandia experiment has the same ramp wave travel through several specimens of different thicknesses, and Backward uses these VISAR measurements to find the stress-strain behavior of the specimen as well as the original loading stress history on the specimens. Details of Backward are given in forthcoming reports[3, 4]. The method starts from a VISAR record and integrates the usual Lagrangian equations of motion backward in space to the interior of the specimen. A description of the flow is obtained in regions where reflections from the VISAR free-surface (or window) interface have not perturbed the flow (as well as an accurate description of regions that are perturbed, which is relevant to the present study). This corrects for the free-surface perturbations in a rather exact way, eliminating a common problem in data interpretation. The original model had the limitation that stress be a single-valued, increasing function of strain. Thus its usefulness was restricted to experiments where the compressive stress is large compared with the yield strength and the latter can be safely ignored. The method was subsequently extended to treat elastic-plastic materials[4].

Backward cannot treat problems with shocks although for some cases the entropy jump across the shock is small enough so that the shock can be treated as an isentropic compression. Errors incurred by this approximation are easily quantified as shown below.

Shock-wave experimentalists routinely measure spall strength of materials by the pullback method[5]. Experimentalists want to deduce the stress history at the spall plane from VISAR data taken at the free surface to develop models for the spall process. Spall strength and yield strength are usually of the same order, so that the consideration of strength effects is mandatory.

The elastic-plastic treatment developed for Sandia applications is inadequate to describe the Los Alamos spall experiment on 6061-T6 aluminum considered in this report. However, we have found that the time-dependent plasticity model known as quasielasticity[6–8] gives a good quantitative description of the one experiment we have analyzed and that the numerical values of the quasielastic parameters are in good agreement with those deduced by Johnson *et al.*[6–8] in the original work on release waves from 200 kbar in 6061-T6 aluminum. This note describes the required modifications to Backward to incorporate quasielasticity and gives results for that one spall experiment. The entire backward method is not described here.

II. THE BACKWARD METHOD

First we define terms as follows:

σ_n normal stress, the stress on the plane of the shock front (without a subscript σ_n is implied).

σ_t transverse stress, the other principal value of the stress tensor. It is the stress on all planes perpendicular to the shock plane. Note that we take σ_n and σ_t to be *positive* in compression. This is contrary to the usual engineering convention.

τ shear stress, $\tau = (\sigma_n - \sigma_t)/2$. This is the maximum shear stress. It occurs on planes tangent to a 45 deg cone around the shock direction.

P mean stress, $P = (1/3)\sigma_n + (2/3)\sigma_t$. The mean stress is also called pressure.

y Lagrangian spatial coordinate. Strips of t-integration are done as Backward develops variables along new y-coordinates.

ν Poisson's ratio.

Y engineering yield strength. It's the normal stress on a rod in a uniaxial stress condition at yield.

ϵ volumetric strain, $\epsilon = 1 - \rho_0 V$.

$f(P)$ a function relating volumetric strain and the mean stress, $\epsilon = f(P)$.

In the Backward solution strategy, the finite difference analogues of the Lagrange equations of motion are solved for the "initial value problem" where the velocity and stress histories are specified at a fixed Lagrangian position (typically the VISAR measurement plane), and the integration proceeds backward in space toward the surface on which the stress load was applied to the specimen under investigation. The momentum conservation, constitutive, and mass conservation equations are[9]:

$$\left(\frac{\partial \sigma_n}{\partial y}\right)_t = -\rho_0 \left(\frac{\partial u}{\partial t}\right)_y, \tag{1}$$

$$V = F(P), \tag{2}$$

$$\left(\frac{\partial u}{\partial y}\right)_t = \rho_0 \left(\frac{\partial V}{\partial t}\right)_y. \tag{3}$$

The original backward formulation proceeded in two stages. It was first done in the fluid approximation and for this case $\sigma_n = P$. It was then extended to an isotropic solid, describable by two elastic constants. The above equations cover this case as well as more general ones.

The equations are each solved along a time line in the following order: momentum conservation to find the stress at the new location, $y + dy$; EOS/constitutive relations to find the strain at the new location, $y + dy$; mass conservation to find the particle velocity at the new location $y + dy$. The entire procedure is repeated until the state variables are calculated at some desired interior position away from the initial location.

For elastic/perfectly plastic materials the time integration at the new position y proceeds as follows:

$$\tau(y, t + dt) = \tau(y, t) + \frac{1 - 2\nu}{1 - \nu} \frac{\sigma(y, t + dt) - \sigma(y, t - dt)}{2}, \tag{4}$$

subject to the following:

$$|\tau(y, t + dt)| \leq Y/2. \tag{5}$$

The latter equation is the von-Mises yield condition. If the inequality (5) is not met when applying Eq. (4), the shear stress is set to $\pm Y/2$, *i.e.*, on the upper or lower yield surface, as appropriate. The new strain is then easily calculated because the mean stress is related to the normal and shear stress:

$$P = \sigma - \frac{4}{3}\tau, \tag{6}$$

and then:

$$\epsilon(y, t + dt) = f\big(P(y, t + dt)\big). \tag{7}$$

For a transcendental f, a predictor/corrector method is required to calculate the new strain to second-order accuracy.

III. EXPERIMENT DESCRIPTION

We analyze a single spall experiment (see Table I). A 2-mm-thick disk of aluminum (the impactor) was thrown at a 4-mm-thick aluminum target using a light-gas gun. The projectile consisted of a thin aluminum case surrounding (except for the impact face) a core of low-density syntactic foam. The impactor was glued to the foam with a thin layer of epoxy. The target was held in a plastic mounting plate using epoxy around the circumference of the target. A single VISAR probe was aimed at the center of the free surface of the target. Light from the VISAR probe was split and sent to two VISARs. The free-surface velocity measured from the two VISARs agrees within about 0.5%. This experiment was designed to produce spall failure at approximately 2 mm from the VISAR measurement surface. The projectile velocity was 0.302 km/s. It had a tilt at impact of about 1 mrad.

TABLE I: **Impactor/Target Data.**

Item	**Material**	**Thickness** (mm)	**Diameter** (in.)	**Density** (g/cm^3)
Impactor	6061 Al	2.015 ± 0.001	1.5	2.707
Target	6061 Al	4.075 ± 0.001	1.25	2.706

IV. ELASTIC/PERFECTLY PLASTIC MATERIAL DESCRIPTION IS NOT ADEQUATE

Calculated stress history, using the elastic/perfectly plastic model, at the spall plane is shown in Fig. 1. This spall location was chosen because it is the plane at which the RMS late-time wiggles in stress are minimized. This general strategy is described in more detail later. The elastic/perfectly plastic model parameters cannot further reduce the RMS of the late-time wiggles in the stress history at the spall plane, no matter how you choose them.

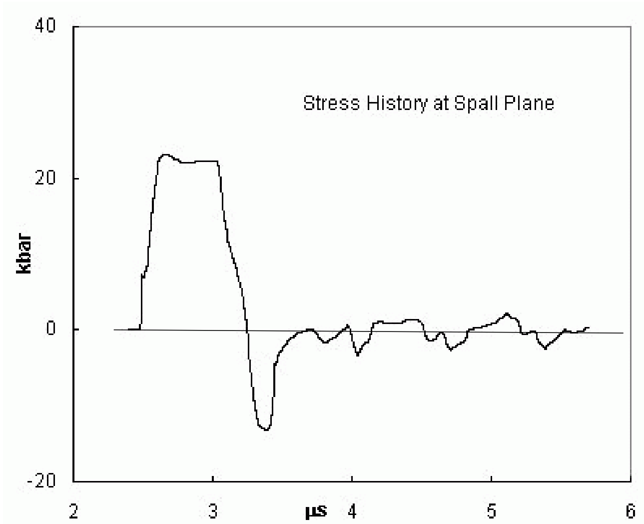

Fig. 1: Stress history at the spall plane for an elastic-plastic model. The stress at the spall plane does not remain small as would be expected for a spall failure.

V. QUASIELASTIC BEHAVIOR

Johnson *et al.* explained anomalies in observed release waves in 6061-T6 aluminum by introducing the notion of quasielastic behavior[6–8]. As shear stress rises or falls, the corresponding strain is not entirely elastic. There are pinned dislocation loops that stretch, providing some reversible plastic strain. In this model, the aluminum release from a shocked state on the upper yield surface is not totally elastic. As the shear stress drops, the pinned dislocation loops migrate back toward their initial locations and eventually reverse. In doing so, they introduce some plastic strain into the "elastic" part of the release. Migration of dislocation loops is thought not to be instantaneous owing to dislocation drag. Thus the equations modeling quasielastic behavior are time dependent and the influence of quasielasticity depends on experiment dimensions and time scales. *This wave propagation effect is likely to be important for those who analyze spall phenomena in small samples.* According to the model, the magnitude of the quasielastic perturbations can be large or small, depending upon the density of pinned dislocations, mobility of the dislocations, and the time scale of the experiment.

We seek to introduce quasielasticity into the backward method and find best values for the quasielastic parameters *and* for the position of the spall. According to Johnson[8]

$$\dot{\beta} \approx (8Gb^2/BL^2)(\tau - \beta), \tag{8}$$

$$\dot{\tau} = G(\dot{\rho}/\rho - \dot{\gamma}_s), \tag{9}$$

$$\dot{\gamma}_s = (b^2 n/B)(\tau - \beta), \tag{10}$$

where τ, ρ, and G are shear stress, density, and shear modulus. The quasielastic "plastic" strain is denoted by γ_s, β is an internal state variable with dimensions of stress, and β falls toward τ exponentially in time. The symbols B, b, L, and n are: viscous drag coefficient, Burger's vector, distance between pinning centers, and line density of pinned dislocations. The reader is referred to the cited paper for details. In the following Backward calculation, the shear stress is calculated with Eqs. (8–10) rather than Eq. (4). We still keep τ within the yield surface, inequality (5). Backward treats the three quantities: b^2n/B, $8(b/L)^2/B$ and X the scab thickness as free parameters and seeks to find values that minimize the RMS of stress oscillations that occur after spall occurs, as should be the case at a newly created spall free-surface. Guesses are made for each of the three parameters and Backward finds the stress history at the candidate spall location, -X. Parameters are varied slightly and another integration done. This procedure is repeated in a systematic way until the RMS of the untoward oscillations on the spall plane is minimized. This is a typical way in which other Backward calculations proceed: guess parameters and improve guesses to minimize some residual between calculation and experiment. Figure 2 shows the VISAR free-surface velocity and the result of a forward integration of the deduced spall history. Figure 3 shows the deduced stress history at the deduced spall location. The RMS of the late oscillations in the Backward calculation is 0.23 kbar or about 1% of the peak stress in the experiment. Minimizations using elastic-plastic had an RMS that was almost an order of magnitude larger. (See Fig. 1.) Figure 4 shows the stress field as a function of space and time and gives a good overall picture of what Backward is doing.

The agreement with Johnson's values obtained by Backward is quite remarkable because Johnson's values (shown in Table II), obtained from releases from 200 kbar, played no role in the Backward determination of the parameters. Apparently, this quasielastic description works well over a rather large range of stress. The other parameters used are given in Table III.

TABLE II: **Johnson and Backward dislocation parameters and the Backward spall thicknesses (cgs units).**

	Johnson	Backward
b^2n/B	1.596×10^{-5}	1.5×10^{-5}
$8(b/L)^2/B$	8×10^{-3}	2.771×10^{-5}
X (cm)	-	0.1994

TABLE III: **Other values required for the calculation.**

EOS parameter	Value	Source
ρ (g/cm^3)	2.703	Fritz data tables
c_0 (cm/s)	5.288×10^5	"
s	1.3756	"
$\rho\gamma$ =constant	2.703×2.14	Handbook
Y (dyne/cm^2)	2.63×10^9	HEL, this expt.
ν	0.344	c_L, c_B, this expt.

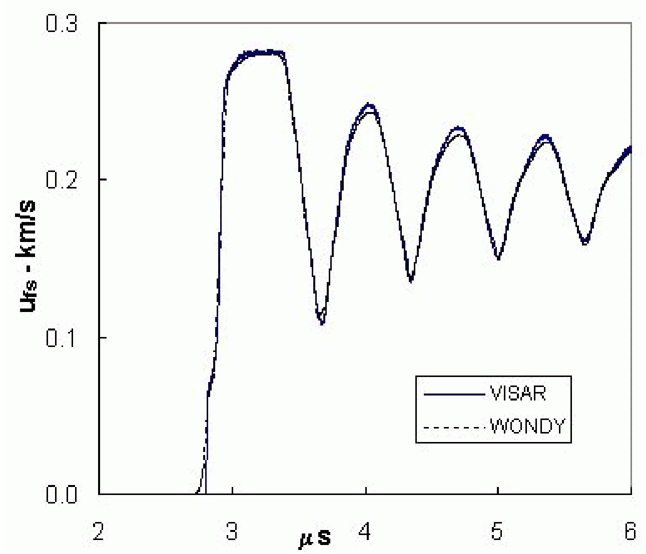

Fig. 2: VISAR record showing pullback from spall followed by ringing in the spall scab. The WONDY calculation used the stress history of Fig. 3, the deduced quasielastic parameters, and the deduced spall thickness to calculate free surface motion.

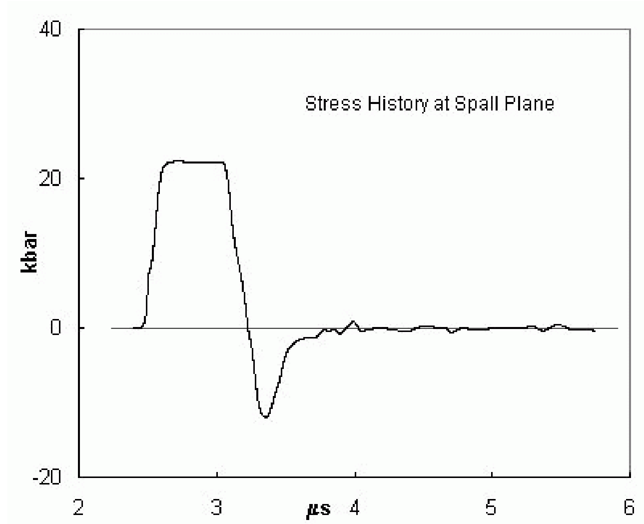

Fig. 3: Calculated stress history at the spall plane using the quasielastic model.

VI. COMMENTS ON THE METHOD

For situations where $f(P)$ is known, it would probably be easier to integrate Eqs. (1-3) using a commercial partial differential equation solver. However, $f(P)$ is often transcendental, and the introduction of strength makes the equations parabolic. Therefore, it is more convenient to use our own numerical procedure.

A general question arises about the numerical stability of these equations. Without strength effects, the entire equation set is hyperbolic, and presumably one can numerically integrate backward and forward in time or space with impunity. But by adding strength, the equations become parabolic in time. The fundamental stability of numerical solutions to these equations has not been determined yet. In lieu of analyzing the stability limit for space steps appropriate to this equation set [for parabolic equations, $dx \propto \sqrt{dt}$], we simply decreased the space step until satisfactory results were consistently achieved. This was about 5% of the equivalent "Courant condition" that prevents disturbance speed from exceeding mesh speed. As a practical matter, when the stress-time history at the spall plane was determined from backward integration of the VISAR record and used as the loading condition to do the forward calculation on a specimen with the scab thickness using a traditional hydrodynamic code, the calculation reasonably replicated the experimental VISAR record. (See Fig. 2)

Sometimes our solutions develop instabilities. In this spall example, stress and particle velocity are smoothed every 25 space steps to suppress these, *e.g.*,

$$\sigma(y,t) \leftarrow \left(\sigma(y,t-dt) + 2\sigma(y,t) + \sigma(y,t+dt)\right)/4. \quad (11)$$

We have determined that smoothing every 10–50 steps has no influence on the ultimate solution for this particular problem. Smoothing well outside these frequency bounds leads to unacceptable errors in the solution.

The calculation of free surface motion in Fig. 2 always replicates the experiment when using this backward/forward technique, even if the material model and the selected spall plane are incorrect. That is because the same equations are being integrated back in space and then forward in time, in effect, just mapping the VISAR record back into itself. Another way of saying this is that the backward integration can be carried back to essentially any location in the interior of the specimen, the stress history at that location used in WONDY[10] for a forward calculation, and the original VISAR record recovered. Conversely, the stress history at the spall plane is sensitive to both material model and to location. The calculated stress history for an E-P material does not remain at zero stress after about 3.6 μs as would be expected for a material that had spalled. We conclude that E-P is not a good material model for 6061-T6 aluminum for the conditions in this experiment. Quasielasticity produced a more satisfactory result.

To recap: zero stress in the solution after spall fixes the free parameters; the forward WONDY calculation matching the VISAR record validates the approximations made in the parabolic backward equations.

Applying this method requires judgment in choosing the time interval for minimizing the late-time wiggles. Slightly different quasielastic parameters are obtained if the time interval is changed.

For this problem, it is not possible to run the entire simulation starting with the initial plate impact. To do so would require a mathematical model for the spall process.

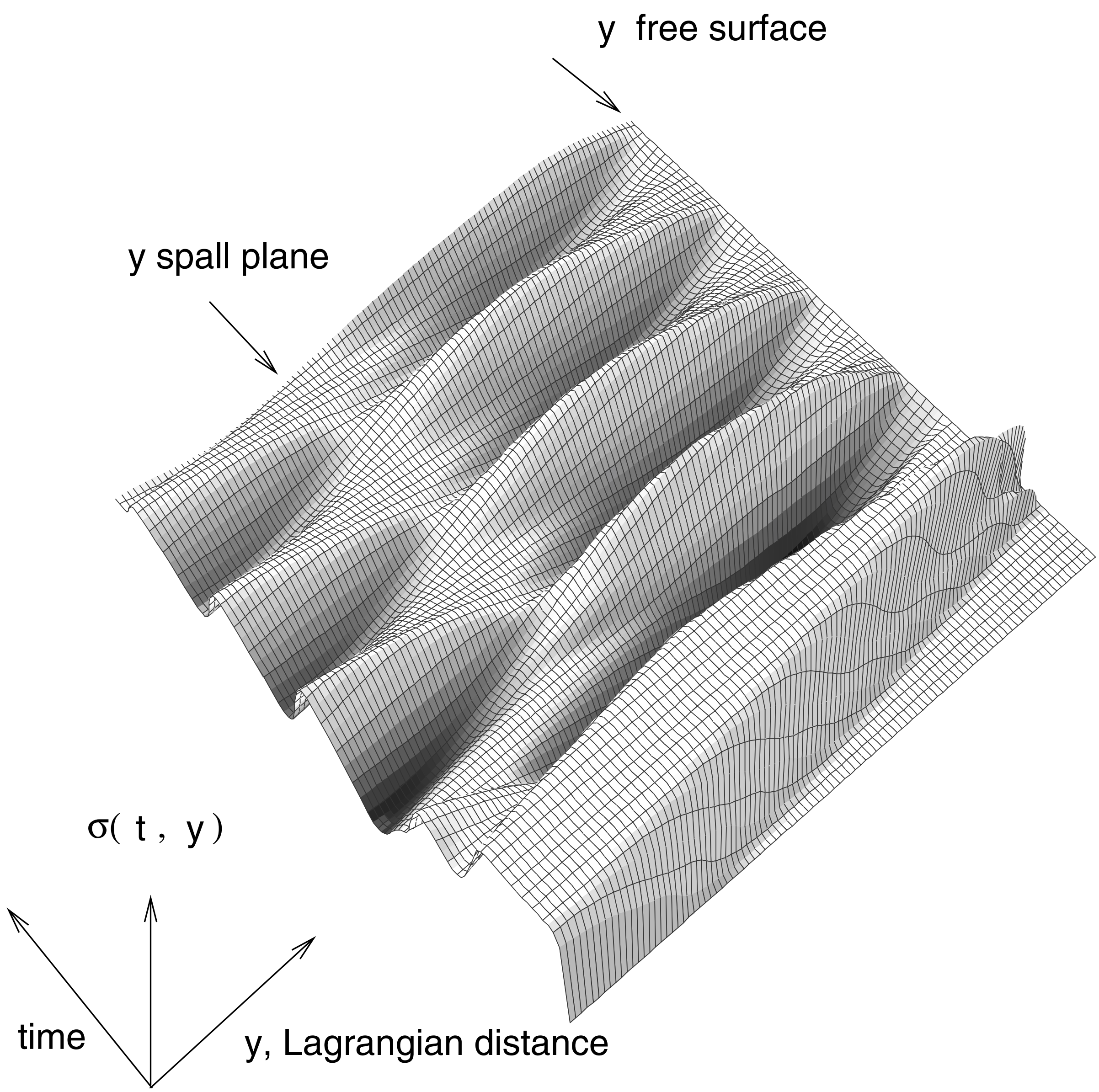

Fig. 4: Experimental determination of the stress field using Backward. The graph shows $\sigma(y,t)$ determined by Backward integration of the equations of motion. The perspective of this 3-D graph was selected so that it resembles the traditional x-t diagrams commonly used in the shock-wave community. Peak stress is about 22 kbar, and minimum stress (the dark trough that is partially obscured in this view) is about -12 kbar. Time increases as indicated. In this particular Backward calculation we choose $y = 0$ at the free surface and integrate toward $y < 0$. Integration was taken to -3 mm depth; the deduced spall plane can easily be seen to be at a depth of about -2 mm. At the spall plane, stress history is the same as the one shown in Fig 3. Initially at the spall plane, stress rises to ≈22 kbar and plateaus. When releases arrive, stress becomes negative and then rises to zero as the aluminum spalls. At the deduced spall plane, the stress is nearly zero for all times after that. Notice that this zero "stress behavior" only occurs at one position. This allows Backward to find the position of the spall. Quasielastic parameters and spall position were varied in a systematic way to achieve the smallest RMS of the stress after spall completion. The stress surface shown here is the one corresponding to the optimum parameters. Other values of those parameters would produce different surfaces (not shown).

VII. CONCLUSION

Direct integration of a VISAR record to deduce the entire motion of a specimen has considerable advantage over more traditional methods for analyzing spall behavior of materials. Results display stress on the spall plane directly, without the use of any particular spall model and therefore should allow evaluation of the various micromechanical spall models that presently exist. We notice that our aluminum record displays a rapid rise in stress followed by a lower rise in stress as zero stress is approached. This "secondary spall" resistance has been seen in tantalum and other materials[11].

The backward method ignores some of the entropy increase from the shock process and will become less valid for strong shocks. Results are validated by taking the deduced stress history at the spall plane and using this as a boundary condition in a more traditional hydrocode forward solution through a layer of scab thickness. If the calculated free-surface motion agrees with the original VISAR record, then the approximation made during the backward integration was valid. The experiment that we analyzed is dissipative due to plastic deformation and the governing equations are therefore parabolic. So information obtained at the rear surface by the VISAR cannot be used by Backward (or any other technique) to determine *with certainty* how the material responded in the sample interior. Unlike the Backward results for hyperbolic problems, the present solutions cannot be considered unique, only highly plausible.

The backward method is finding application to a variety of problems[3]. It holds the promise of giving a new window into strength and release behavior in materials that is not possible with traditional analysis techniques. Sweeping away some of the complications of wave propagation from an experiment permits a more direct look at some physical processes of interest.

REFERENCES

[1] L. M. Barker and R. E. Hollenbach, *J. Appl. Phys.* **43**, 4669 (1972).

[2] C. Hall *et al.*, submitted to *Rev. Sci. Instrum.* (2001).

[3] D. B. Hayes, *Backward Integration of the Equations of Motion to Correct for Free Surface Perturbations*, Sandia National Laboratories Report SAND2001-1440, (2001).

[4] D. B. Hayes, *Correcting free-surface perturbations by integrating the equations of motion backward in space*, submitted to APS Topical Conference on Shock Compression in Condensed Media, Atlanta, Georgia (2001).

[5] T. H. Antoun, L. Seaman, and D. R. Curran, *Dynamic Failure of Materials Volume 1—Experiments and Analyses*, SRI International Report DSWA-TR-96-77-V1, (1998), p. 122.

[6] J. N. Johnson, P. S. Lomdahl, and J. M. Wills, *Acta Metall. Mater.* **39**(12), 3015 (1991).

[7] J. N. Johnson, R. S. Hixson, G. T. Gray, III, and C. E. Morris, *J. Appl. Phys.* **72**(2), 429 (1992).

[8] J. N. Johnson, *J. Phys. Chem. Solids* **54**(6), 691 (1993).

[9] We make slight changes in the notation from the SAND report to emphasize the Lagrange nature of these equations. We use y for the Lagrange coordinate instead of x, which usually refers to an Eulerian coordinate. We use an overhead dot for $(\partial\ /\partial t)_y$. This convention has some justification because this particular time derivative is the full time-derivative of a particular particle.

[10] M. E. Kipp and R. J. Lawrence, *WONDY V - A One-Dimensional Finite-Difference Wave Propagation Code*, Sandia National Laboratories Report SAND81-0930, (1982).

[11] A. K. Zurek, W. R. Thissell, J. N. Johnson, D. C. Tonks, and R. S. Hixson, *Journal of Materials Processing Technology* **60**, 261 (1996).

Los Alamos
NATIONAL LABORATORY

Los Alamos, New Mexico 87545